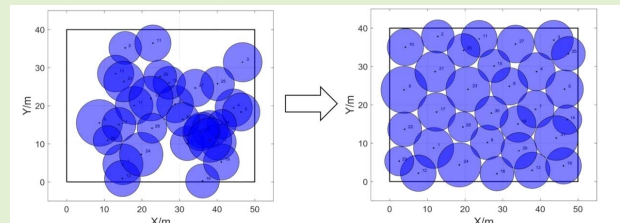


Coverage Enhancement Algorithm for WSNs Based on Vampire Bat and Improved Virtual Force

Qin Wen^{ID}, Student Member, IEEE, Xiao-Qiang Zhao^{ID}, Yan-Peng Cui^{ID}, Student Member, IEEE, Yao-Ping Zeng, Hong Chang, and Yin-Juan Fu

Abstract—Coverage enhancement is an important strategy to avoid coverage holes caused by the random deployment of sensor nodes. Given the harsh physical environments of wireless sensor networks (WSNs), which impede the energy supplement and recovery of sensor nodes, the motivation of our research is to repair the coverage holes and reduce the energy consumption during the deployment of sensor nodes. Firstly, by using cellular grids to stack the monitoring area, a bipartite graph model between the nodes and the cellular grids is constructed to minimize and balance the moving distance during the redeployment. Secondly, the vampire bat algorithm is introduced for bipartite graph matching. Finally, the coverage effect and moving distance are further optimized based on the improved virtual force. The simulation results show that the coverage rate is increased by 5.43%, 3.25%, and 1.63%, and the moving distance is reduced by 33.64%, 3.66%, and 2.01% when compared with COSH, VF-IALO, and HA, respectively. In addition, the proposed algorithm shows good performance in terms of uniformity of moving distance and maximum moving distance.

Index Terms—Wireless sensor networks (WSNs), vampire bat algorithm, improved virtual force, coverage enhancement and moving distance optimization.



I. INTRODUCTION AND RELATED WORKS

THE paradigm of wireless sensor networks (WSNs) involves a large number of sensor nodes, which are capable of performing complicated sensing tasks in a specific field cooperatively without any human interaction [1]. In recent years, with the development of automation technology, distributed information processing technology, and embedded

Manuscript received February 15, 2022; accepted March 11, 2022. Date of publication March 14, 2022; date of current version April 14, 2022. This work was supported in part by the National Nature Science Foundation of China under Grant U1965102, in part by the Science and Technology Innovation Team for Talent Promotion Plan of Shaanxi Province under Grant 2019TD-028, in part by the Key Research and Development Project of Shaanxi Province under Grant 2020NY-161 and Grant 2020GY-056, and in part by the Science and Technology Achievement Transfer and Extension Plan Absorption Achievement Transformation Project of Shaanxi Province under Grant 2020CGXNG-014. The associate editor coordinating the review of this article and approving it for publication was Prof. Jaime Lloret. (Corresponding author: Yan-Peng Cui.)

Qin Wen, Xiao-Qiang Zhao, Yao-Ping Zeng, Hong Chang, and Yin-Juan Fu are with the Shaanxi Key Laboratory of Information Communication Network and Security, and the School of Communication and Information, Xi'an University of Posts and Telecommunications, Xi'an 710121, China (e-mail: wq199802@163.com; zxq7703@126.com; zengyp03@163.com; nuc_changhong@126.com; ffuyinjuan@163.com).

Yan-Peng Cui is with the Key Laboratory of Universal Communications, Ministry of Education, Beijing University of Posts and Telecommunications, Beijing 100876, China (e-mail: cuiyanpeng94@bupt.edu.cn).

Digital Object Identifier 10.1109/JSEN.2022.3159649

technology, WSNs have been widely applied in environmental monitoring [2], emergency communication [3], intelligent agriculture [4], and other fields.

The area coverage reflects the perception of WSNs to the surrounding environment, where a good coverage effect can ensure effective data collection [5]. The coverage is usually enhanced by redeploying the sensor nodes as they tend to deviate from the optimal location upon random deployment. The sensing radius between the nodes is different with the interference of harsh and complex environments, e.g. white noise [6], humidity [7], and path loss [8]. For example, in the water environment, for signals transmitted from a far-field, the sensing radius between nodes affected by path loss, surface noise, or large propagation delays, is different [9], [10]. In addition, the internal thermal noise, power consumption, and residual energy of sensors also affect the sensing accuracy [6], [11]. How to deploy nodes based on the difference in sensing radius is the key to the coverage enhancement.

Given the limitation of the recharging and restoration of the batteries of the nodes, energy should be the top consideration in WSNs [12]. Therefore, the intention of our research is to enhance the coverage and reduce energy consumption during the redeployment.

As the most effective coverage enhancement algorithm, the virtual force algorithm (VFA) was proposed and improved

TABLE I
COMPARISON OF RELATED WORKS

	[13]	[14]	[15]	[16]	[17]	[18]	[19]	[20]	[21]	[22]	[23]	[24]	[25]	[26]	[27]	Proposed
Force-Based	✓	✓		✓		✓	✓	✓								✓
SI-Based								✓	✓	✓	✓	✓	✓	✓	✓	✓
Grid Division									✓							✓
Geometric-Based	✓	✓	✓	✓	✓	✓	✓		✓	✓				✓	✓	✓
Coverage Effect	✓	✓	✓	✓	✓	✓	✓	✓	✓	✓	✓	✓	✓	✓	✓	✓
Moving Distance(MD)	✓	✓	✓	✓	✓	✓	✓	✓	✓	✓						✓
Uniformity of MD								✓		✓						✓
Time Consumption			✓	✓					✓	✓	✓	✓		✓	✓	✓
Delivery Ratio											✓	✓				
Difference in Sensing					✓	✓								✓	✓	
Obstacle	✓						✓									

by many scholars. By defining the virtual force of uncovering grids and sensors based on a geometric relationship, an improved VFA was proposed in [13], which can effectively improve the coverage rate of WSNs. The work of [14] proposed an adaptive VFA by setting the best parameters of attractive and repulsive force in different environments, which can optimize the coverage effect and improve the adaptability of VFA. Liao *et al.* [15] transformed the coverage enhancement into a weighted bipartite graph matching problem, and introduced the extended Hungary algorithm (HA) for minimizing the moving energy consumption of nodes. In [16], a multiplicatively weighted Voronoi was proposed by defining the vertex virtual force and edge virtual force of the Voronoi diagram, which increased the robustness of VFA. In order to optimize the moving distance and ensure the coverage effect, Du *et al.* [17] proposed a coverage optimization algorithm based on the sampling for heterogeneous WSNs (COSH) by analyzing the geometric relationship between the intersection of sampling lines and sensing disks with different radius. By setting the resultant of force exerted on sensors based on the ratio of sensing range, the work of [18] proposed an improved force-based deployment algorithm, which can maximize the coverage while reducing the moving distance. Luo *et al.* [19] proposed a 3-D virtual force coverage algorithm, which can improve the coverage rate and reduce the large moving distance caused by node blind movements. Although the coverage enhancement strategy geometric-based shows good performance in terms of energy optimization and convergence speed, it is difficult to find the optimal distance threshold between the nodes, which results in an upper limit of coverage [20].

As an efficient algorithm for solving optimization problems, swarm intelligence (SI) has been applied widely in the coverage enhancement of WSNs also. By setting dynamic weighting coefficients for the virtual force and ant lion, the virtual force-directed improved ant lion optimization algorithm (VF-IALO) was proposed by Yao *et al.* [20], which could effectively improve the coverage rate and accelerate the convergence speed. In order to improve the convergence speed, a vector force augmented biogeography-based optimization (BBO) was proposed in [21] by embedding virtual force into BBO. Based on the Boolean sensing model, Zhao *et al.* [22] transformed the coverage enhancement problem into a task assignment problem between the nodes and truncated octahedron.

Besides, according to the biological characteristics of the vampire bats, the vampire bat algorithm (VBA) based on the game theory was proposed to optimize the coverage effect, and also to minimize and balance the cost of redeployment of sensor nodes. As a classical article in the coverage of WSNs, ant colony optimization(ACO) is a good choice to deal with the hole problem of WSNs. Saleem *et al.* [23] studied the capability of an ACO-based routing protocol, called the biologically inspired secure autonomous routing protocol(BIOSARP), which can efficiently maintain the network communication. The author in [24] extended the analysis to the study of the scalability and stability of BIOSARP to handle the holes problem. In [25], the maximum number of monitored targets in WSNs was obtained by combining glow-worm swarm optimization (GSO) and the merits of a clone generator. A Particle swarm optimization-inspired probability algorithm was proposed by Morsly *et al.* [26], which ensured the utilization of the minimum number of sensors to achieve accurate coverage. In [27], an efficient genetic algorithm for maximum coverage deployment was proposed, which ensured the nodes are evenly distributed in the monitoring area by introducing genetic algorithm to update positions iteratively. The coverage enhancement based on SI considers mainly the coverage effect as an objective of optimization while ignoring the total moving energy consumption and the uniformity of moving energy consumption [22]. The contribution of our proposed strategy with existing methods is compared in Table I.

In the paper, we propose a coverage enhancement algorithm for WSNs based on vampire bat and improved virtual force (VB-IVFA). The major contributions of our research are as follows:

- 1) A division strategy based on cellular gird is proposed for monitoring area. The coverage enhancement and energy optimization problem of nodes with different sensing radii is transformed into a bipartite graph matching problem and solved by VBA for the first time.
- 2) The causes of coverage holes after assignment are analyzed, and an improved virtual force algorithm (IVFA) is proposed.
- 3) The parameters in IVFA are numerically analyzed to ensure the coverage effect and optimize the mobile energy consumption.
- 4) The performance of VB-IVFA is simulated and compared with COSH, VF-IALO, and HA in terms of the

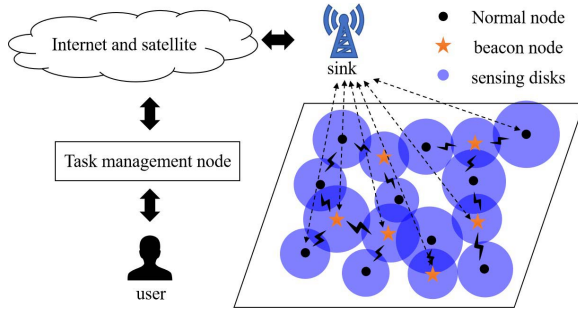


Fig. 1. Coverage model.

coverage rate, energy consumption, etc. We also analyze the reasons for the difference in performance.

The rest of the paper is organized as follows. The coverage problem model and evaluation indicators are described in Section II. In Section III, we present the cellular grids division strategy and coverage enhancement strategy based on VBA. In Section IV, we analyze the reasons for coverage holes and propose IVFA. We perform numerical analysis on the key parameters of IVFA, and show the experimental results and analysis in Section V. Finally, we summarize the paper and look forward to the research in the future.

II. PROBLEM STATEMENT

Coverage enhancement and energy consumption optimization are two core issues during the redeployment of WSNs. In this section, we will illustrate the coverage model and describe the evaluation indicators of coverage enhancement.

A. Coverage Model

We consider a WSNs of N sensor nodes in the monitoring area $L \times W$ without any obstacles. As shown in Fig. 1, there is a control center (e.g., a sink), which collects sensors' location information and broadcasts their movement orders to the sensors. Considering the interference of noise (e.g. white noise or internal thermal noise), environment (e.g. humidity or propagation path), and power consumption on the received signal, to reflect the uncertainty and difference of sensing ability between nodes, this paper assumes that the sensing radii of the nodes of the WSNs satisfy the normal distribution $N(R_0, \delta^2)$, where R_0 is the average sensing radius (i.e., the rated sensing range) and δ is the standard deviation [28], [29].

Remark 1: We assume that all the nodes can achieve accurate positioning by using advanced positioning algorithms [30], and send the location information to the control center based on the preset routing protocol [31]. We choose not to discuss them in this article, for the purpose of avoiding alleviating from the focus of coverage enhancement to positioning and routing.

B. Evaluation Indicators

Coverage effect and moving distance are two important indicators during node redeployment, which are respectively shown as follows.

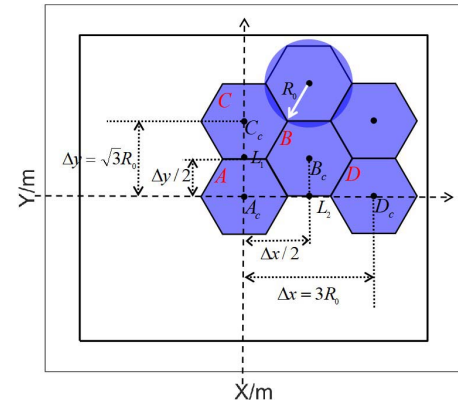


Fig. 2. Cellular grid division.

1) Coverage Rate (COVR): In order to calculate the COVR of WSNs, the monitoring area is divided into $m \times n$ grids. The Euclidean distance between the centroids of grid C_j and node S_i is expressed as $\|C_j, S_i\|$. The probability of C_j being sensed successfully by S_i is:

$$P(C_j, S_i) = \begin{cases} 1, & \|C_j, S_i\| \leq R_i \\ 0, & \|C_j, S_i\| > R_i, \end{cases} \quad (1)$$

where R_i is the sensing radius of S_i . A grid will be covered successfully once it is sensed by any node, which is expressed as p_{C_j} . The COVR of WSNs can be calculated as $P = \sum_{j=1}^{m \times n} p_{C_j} / m \times n$.

2) Moving Distance: Energy consumption during redeployment mainly results from moving and signal transmission, and the former is of great importance than the latter for mobile nodes [22]. Therefore, the energy consumption of sensor is measured in terms of moving distance of nodes. After redeployment, the total moving distance (TMD) of the nodes is expressed as $D_{TO} = \sum_{i=1}^N d_i$, where N is the number of nodes and d_i is the moving distance during the redeployment of S_i . The uniformity of moving distance (UMD) is defined as $D_{Uni} = \sqrt{\sum_{i=1}^N \left(d_i - \frac{D_{TO}}{N}\right)^2}$. The maximum moving distance (MMD) is expressed as $D_{max} = \max_{i=\{1,2,\dots,N\}} \{d_i\}$.

III. GRID DIVISION AND VAMPIRE BAT ALGORITHM

Efficient grid division of the monitoring area is not only capable to ensure the uniform distribution of nodes, but also enhances the COVR with the fewest nodes. In this section, the coverage enhancement and energy optimization problem is transformed into a bipartite graph matching problem by cellular grid division, which is then optimized by VBA.

A. Cellular Grid Division

Determination of the optimal deployment of nodes without any difference in sensing radius is equivalent to finding a regular polygon with the highest stacking efficiency. The cellular grid has the highest stacking efficiency, which is often regarded as the best deployment of two-dimensional area [32]. In order

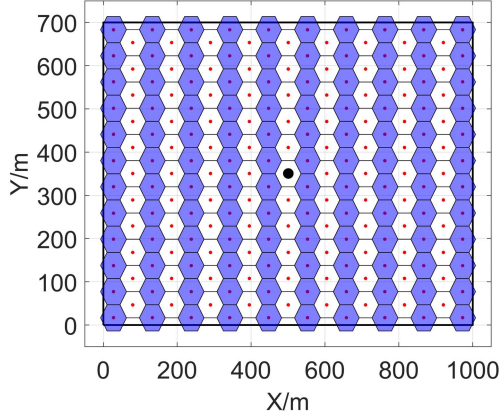


Fig. 3. Effect of cellular grid division of monitoring area $700m \times 1000m$.

to ensure the uniform distribution of nodes after redeployment, this paper takes the average sensing radius of all the nodes as the circumscribed circle radius of the cellular grids. As shown in Fig. 2, the cellular grid A , whose centroid is denoted as A_c , in the center of the monitoring area is taken as the benchmark. Since there exist geometric relations of $|\overrightarrow{A_c L_1}| = \Delta y/2 = \sqrt{3}R_0/2$, $|\overrightarrow{A_c C_c}| = \Delta y = \sqrt{3}R_0$, $|\overrightarrow{A_c L_2}| = \Delta x/2 = 1.5R_0$, $|\overrightarrow{A_c D_c}| = \Delta x = 3R_0$, the centroidal coordinate B_c of the cellular grid B becomes $(1.5R_0, \sqrt{3}R_0/2)$. Therefore, given the monitoring area $L \times W$ and sensing radius R_0 , the fewest number of cellular grids required in the following steps:

Step 1: Since the distance between the centroid A_c of the cellular grid A and the right (upper) edges of the monitoring area is $L/2$ ($W/2$), the minimum number of cellular grids required in the X and Y directions are:

$$\begin{cases} N_1 = 2 \times \lfloor L/2/\Delta x \rfloor + 1 \\ N_2 = 2 \times \lfloor W/2/\Delta y \rfloor + 1, \end{cases} \quad (2)$$

Step 2: Since the distance between the centroid B_c of the cellular grid B and the right (upper) edges of the monitoring area is $L/2 - \Delta x/2$ ($W/2 - \Delta y/2$), the minimum number of cellular grids required in the X and Y directions are:

$$\begin{cases} N_3 = 2 \times \lfloor (L/2 - \Delta x/2)/\Delta x + 1 \rfloor \\ N_4 = 2 \times \lfloor (W/2 - \Delta y/2)/\Delta y + 1 \rfloor, \end{cases} \quad (3)$$

Step 3: The minimum number of cellular grids required is $N = N_1 N_2 + N_3 N_4$.

When the size of the monitoring area is $1000m \times 700m$ and the radius of the circumscribed circle of the cellular grid is $R_0 = 35m$ [5], the fewest cellular grids required becomes 219 as per the above calculating steps. The effect of the division is shown in Fig. 3.

The coverage enhancement problem can be transformed into a bipartite graph matching problem, in which the nodes move to the centroid of the cellular grids. The efficiency matrix of

the bipartite graph is:

$$Eff_{N \times N} = \begin{bmatrix} d_{1,1} & \dots & d_{1,N} \\ \vdots & \ddots & \vdots \\ d_{N,1} & \dots & d_{N,N} \end{bmatrix} \quad (4)$$

where $d_{i,j}$ is the distance from node S_i to the centroid of the cellular grid G_j . The objective function is defined in terms of the moving distance of the nodes during the redeployment as $\min(f_1 + f_2)$, where f_1 and f_2 are the functions that consider TMD and UMD, respectively. These can be defined specifically as:

$$\begin{cases} f_1 = \frac{1}{N} \sum_{i=1}^N \sum_{j=1}^N d_{i,j} \times x_{i,j} \\ f_2 = \sqrt{\frac{1}{N} \sum_{i=1}^N \sum_{j=1}^N (d_{i,j} \times x_{i,j} - f_1)^2}, \end{cases} \quad (5)$$

The constraints are expressed as:

$$s.t. \begin{cases} \sum_{i=1}^N x_{i,j} = 1, & j = 1, 2, \dots, N \\ \sum_{j=1}^N x_{i,j} = 1, & i = 1, 2, \dots, N \\ x_{i,j} = \begin{cases} 1, & G_j \text{ is the destination of } S_i \\ 0, & \text{otherwise,} \end{cases} \end{cases} \quad (6)$$

B. Vampire Bat Algorithm

Aiming at the problem of minimizing and balancing the moving distance described in (5) and (6), we proposed a novel bipartite graph matching algorithm inspired by the egoistic and altruistic behaviors of vampire bats. The egoistic behavior refers to that process of predation where a vampire bat gets its own interest value for each target prey according to its own hungry level and hunting risk, and selects the target prey according to the degree of interest for predation competition. However, all vampire bats cannot get enough blood in the predation competition. The altruistic behavior indicates that most vampire bats will share their excess blood with a starving bat based on their genetic similarity [33]. For the general binary graph matching problem, the vampire bats algorithm mainly includes the following steps:

Step 1: Parameter initialization. Calculate the benefits of each vampire bat by capturing each prey. For example, the benefit of vampire bat b_i capturing prey p_j at the t -th iteration is $B_{i,j}^t = I_{i,j}^t - r_j^t$, where $I_{i,j}^t$ and r_j^t are the corresponding interest value and hunting risk value, respectively.

Step 2: Find the prey for which each vampire bat is most interested. The most interesting prey of a vampire bat is selected as $p_{best for b_i} = \arg \max_{o \in \{1, 2, \dots, N\}} B_{i,o}^t$.

Step 3: Determine whether any predation conflict takes place between vampire bats due to the interest of different vampire bats for the same prey. Proceed to *step 5* if the most interesting prey of any vampire bat does not conflict. Otherwise, proceed to *step 4*. The conflicting prey is denoted as the hot prey, and the conflicting bats are denoted as the conflict bats.

Step 4: Predation competition. The interest value of vampire bat b_i to hot prey p_a is updated as $I_{i,a}^{t+1} = I_{i,a}^t - (\varphi_1^t - \varphi_2^t + \varepsilon)$, where φ_1^t and φ_2^t are, respectively, the maximum and secondary interest values of all b_i competing for p_a at the t -th iteration, ε is the mandatory updating factor to ensure that the renewal of

the interest value of b_i to p_α can proceed successfully. After the predation competition, return to *step 1*.

Step 5: Predation. There is no conflict between the vampire bats after several rounds of predation competition, and they begin to absorb blood. So far, the benefits of the vampire bat population are maximized. However, every vampire bat cannot get enough blood due to the difference in the amount of blood absorbed by them. Therefore, after predation, all the vampire bats will seek starving vampire bats for back feeding, which is called altruistic behavior.

Step 6: Traverse all vampire bats. Determination of other vampire bats that satisfy the back feeding conditions for vampire bat b_i according to (7).

$$\begin{cases} z_j - z_i > \tau_1 \\ |g_i - g_j| < \tau_2, \end{cases} \quad j \in \{1, 2, \dots, N\}, \quad (7)$$

where z_i and z_j denoted, respectively, the amount of blood absorbed by b_i and b_j after predation; g_i and g_j are, respectively, the genetic values of b_i and b_j ; and τ_1 and τ_2 , respectively, refer to the thresholds to measure the degree of hungry and genetic similarity between b_i and b_j . If multiple vampire bats satisfy the back feeding condition, the genetic similarity and the degree of hungry are comprehensively considered to determine the back feeding prey. For example, if b_j satisfies the back feeding conditions of b_i , which is called as the candidate back feeding bat of b_i , the fitness value of b_j is calculated as:

$$fit_{i,j} = \frac{(z_i - z_j) / \sum_{k=1}^{C_i} (z_i - z_k)}{|g_i - g_j| / \sum_{k=1}^{C_i} (g_i - g_k)}, \quad (8)$$

where C_i is the number of all candidate back-feeding vampire bats of b_i . The vampire bat with the highest fitness value is selected as the best back-feeding prey among all the candidates. The algorithm will end when no bat of the population will satisfy the back feeding conditions. So far, the predation benefits of the entire group of vampire bats have been maximized and balanced.

C. Coverage Enhancement Strategy Based on VBA

As mentioned above, the egoistic behavior of VBA is utilized to solve the maximum matching problem of a bipartite graph. The efficiency matrix of (4) belongs to the minimum matching problem, and hence it can be transformed as $Eff_{N \times N} = -Eff_{N \times N}$. Specifically, the sensor nodes and the centroid of the cellular grids are regarded as vampire bats and prey, respectively. The multi-objective optimization problem of minimizing and balancing the moving distance is solved based on VBA. The coverage enhancement strategy based on VBA mainly includes the following steps:

Step 1: Determine the best cellular grid for each node. For example, the best cellular grid G_j for node S_i at the t -th can be determined as $G_{bestforS_i}^t = \arg \max_{j \in \{1, 2, \dots, N\}} Eff_{i,j}^t$.

Step 2: Competition. If there is no conflict in the best cellular grids for any node, the moving task matrix is calculated as $Task_{N \times N}^t = Eff_{N \times N}^t \Theta X_{N \times N}^t$, where Θ is the Hadamard product operator, and $X_{N \times N}^t$ is the mobile indicator matrix obtained by (6). If any conflict exists between the best

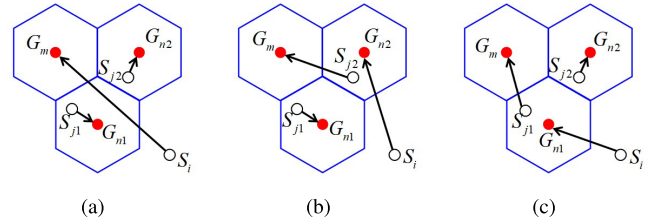


Fig. 4. (a), (b), and (c) represent the redeployment effect before the moving task exchange, exchange approach one, and exchange approach two, respectively.

cellular grids for a node, then the conflicting grids at the t -th iteration are recorded as the hot cellular grid set Φ_{grid}^t , and the corresponding nodes are recorded as the conflicting nodes. For example, if the cellular grid G_α belongs to the hot cellular grid set Φ_{grid}^t at the t -th iteration, the nodes competing for the cellular grid G_α are denoted as $\Phi_{S_{forG_\alpha}}^t$. The benefits of S_i for G_α at the t -th iteration will be updated as $Eff_{i,\alpha}^{t+1} = Eff_{i,\alpha}^t - (\varphi_1^t - \varphi_2^t + \varepsilon)$ once S_i belongs to $\Phi_{S_{forG_\alpha}}^t$, where φ_1^t and φ_2^t are, respectively, the maximum and secondary benefits of the nodes in $\Phi_{S_{forG_\alpha}}^t$ moving to G_{alpha} . ε is the mandatory updating factor, which is used to ensure that the conflicting nodes can update the benefits of the best cellular grid successfully. Update the benefits of each conflicting node to the hot cellular grid in turn and return to *Step 1* until all the nodes find the best cellular grid that no longer conflicts.

Step 3: Exchange the moving task of all the nodes. After *Step 1* and *Step 2*, the TMD of the nodes of WSNs can be minimized. In order to further balance the moving distance, the redeployment task of node is exchanged based on the altruistic behavior of vampire bats. Specifically, S_i and S_j , having their best cellular grids of G_m and G_n , respectively, can exchange their moving tasks once the following conditions are satisfied:

$$\begin{cases} Eff_{i,n} < Eff_{i,m} \\ Eff_{j,m} < Eff_{j,n}, \end{cases} \quad (9)$$

If multiple sensor nodes satisfy the moving task exchange condition of S_i , taking S_j as an example, then the fitness value is calculated as follows:

$$fit_{i,j} = Eff_{i,n} + Eff_{j,m} + |Eff_{i,n} - Eff_{j,m}|, \quad (10)$$

The node with the minimum fitness is regarded as the best exchangeable node.

As shown in Fig. 4, both S_{j1} and S_{j2} satisfy the exchange condition of S_i . Compared with S_{j2} , S_{j1} has a smaller fitness according to (10). Therefore, compared with exchange approach one, exchange approach two can achieve a more balanced deployment with a lesser moving cost. The moving task exchange will be over if no node satisfies the exchange condition anymore. So far, the TMD and UMD are optimized, which is equivalent to the vampire bat population maximizing and balancing the amount of blood drawn.

IV. IMPROVED VIRTUAL FORCE ALGORITHM

The coverage enhancement strategy based on VBA, as explained in Part III, initially improves the COVR of WSNs.

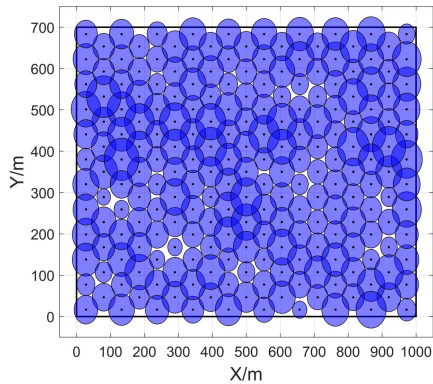


Fig. 5. Coverage effect based on cellular grid division and VBA.

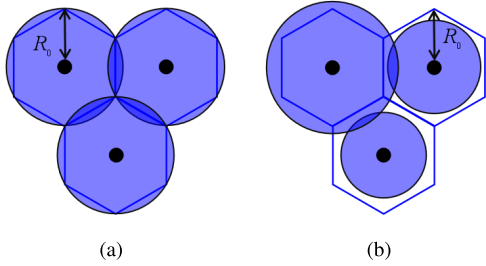


Fig. 6. Coverage effect of cellular grid. (a), (b), respectively, are the coverage effect of nodes with the same sensing radius and different radii.

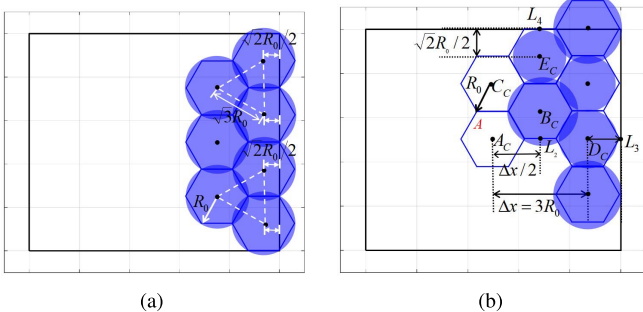


Fig. 7. Coverage effect at boundary. (a), (b), respectively, are the uncovered holes and the covered holes at boundary.

However, there are still coverage holes in the monitoring area due to the variation in the sensing radius as shown in Fig. 5. The coverage holes are generated between the centroid of cellular grids and the boundary of the monitoring area.

1) Between the Centroid of Cellular Grids: If all the nodes have the same sensing radius according to the geometric relationship in Fig. 6(a), the coverage overlap between the nodes is the smallest, and there is no coverage hole at the junction of the three nodes. If all the nodes have different sensing radii, the nodes whose sensing radius is less than R_0 cannot achieve full coverage of the cellular grid, which results in coverage holes, as shown in Fig. 6(b).

2) The Boundary of Monitoring Area: The average sensing radius R_0 is taken as the circumscribed circle radius of the cellular grid, if all nodes have the same sensing radius, taking the right edge of the monitoring area as an example, according to the geometric relationship in Fig. 7, when the distance between the centroid of the cellular grids at the boundary and

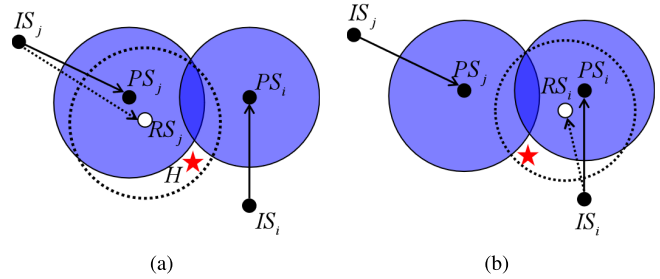


Fig. 8. Redeployment strategy for coverage hole H under different repairing approaches. (a) and (b) show the repairing approach one and repair approach two, respectively.

the boundary is $\sqrt{2}R_0/2$, the coverage holes at the boundary can be completely covered, and the coverage area outside the monitoring area can be minimized. If all nodes have different sensing radii, the following causes that lead to coverage holes. On the one hand, based on the grid division strategy in Part III, the relationship between the size of the monitoring area and the sensing radius of the node is difficult to ensure the distance between the centroid of the cellular grid at the boundary and the boundary is less than or equal to $\sqrt{2}R_0/2$ (e.g., $|\overrightarrow{DC_L3}| > \sqrt{2}R_0/2$ in Fig. 7(a)). On the other hand, even if the distance between the centroid of the cellular grid and boundary is less than or equal to $\sqrt{2}R_0/2$, coverage holes will also be generated due to the difference in sensing radius (e.g., the cellular grid E_C in Fig. 7(b)). Hence, in this section, IVFA is proposed to optimize the COVR and TMD.

A. Virtual Force of Uncovered Grids

In order to repair the coverage holes, a virtual attractive force as shown in (11) is defined between the uncovered grids and nodes. Specifically, for node S_i , d_{ij} is the Euclidean distance between S_i and uncovered grid C_j , and $\theta_1(i, j)$ is the direction angle from S_i to C_j . When the distance between the node and uncovered grid is less than $\sqrt{3}R_0$, the virtual attractive force increases with decreasing distance between them.

$$F_{AS-C}(i, j) = \begin{cases} \left(\frac{1}{d_{i,j}}, \theta_1(i, j) \right), & d_{i,j} < \sqrt{3}R_0 \\ 0, & \text{otherwise,} \end{cases} \quad (11)$$

The total force generated by uncovered grids can be expressed as $F_{AS}(i) = \sum_{j=1}^{num} F_{AS-C}(i, j)$, where num is the number of uncovered grids.

B. Distance Virtual Force

Considering the difference in the sensing radius, the position of the coverage holes generated by the VBA-based coverage enhancement strategy is full of randomness. In order to control the consumption of extra moving energy caused by the virtual force of the uncovered grids, nodes are affected by the distance virtual force.

As shown in Fig. 8, IS_i and PS_i are, respectively, the initial and current positions of node S_i . The coverage hole is represented by H , and RS_i is the position where S_i is ready

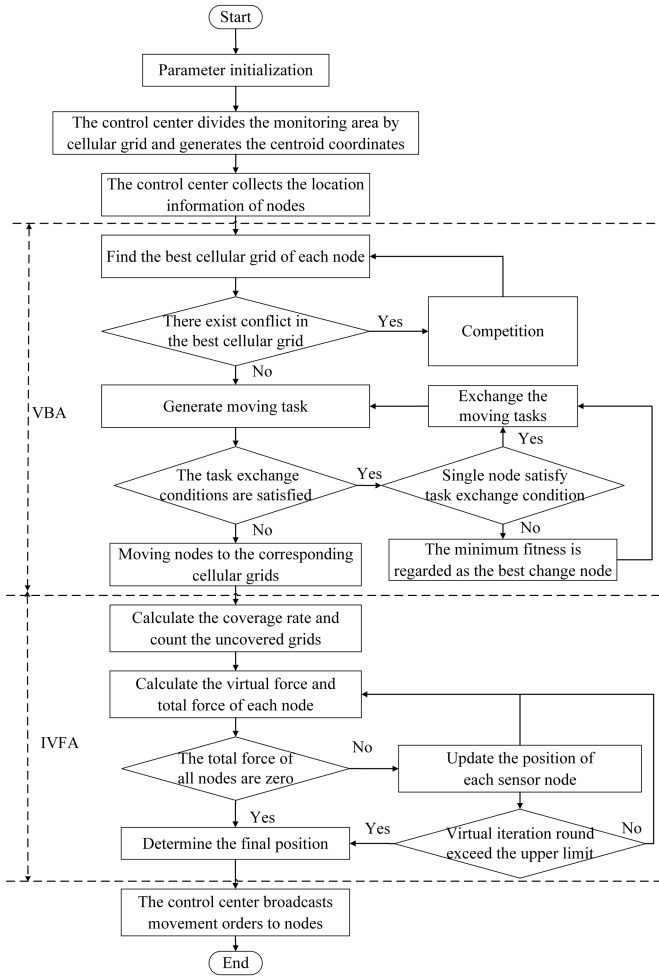


Fig. 9. Flow chart of VB-IVFA.

to move under the uncovered grid virtual force. As shown in Fig. 8(a), both S_i (as shown in Fig 8(a) under the repairing approach one) and S_j (as shown in Fig. 8(b) under the repairing approach two) can repair the coverage hole H . However, compared with S_i , S_j will increase the extra moving distance in repairing the coverage hole H . Therefore, the distance virtual force is proposed to further limit the moving distance when the node is subjected to the uncovered grid virtual force. The distance virtual force is defined as:

$$FB_S(i) = \exp\left(-\frac{1}{d_{IS-PS}(i)}\right), \quad (12)$$

For node S_i , d_{IS-PS} represents the Euclidean distance between the initial and current positions. The direction angle $\theta_2(i)$ from the current position to the initial position. The distance virtual force increases with increasing distance between the two.

C. The Basic Frame of VB-IVFA

The basic framework of the coverage enhancement algorithm for WSNs based on vampire bat and virtual force is shown in Fig. 9. The main steps are as follows:

Step 1: Initialize the sensing radius, position of sensor nodes, virtual iteration rounds and step length of a single iteration.

Step 2: The control center divides the monitoring area by cellular grids and generates the centroidal coordinates.

Step 3: The control center collects the location information of the nodes.

Step 4: Based on the egoistic behavior and altruistic behavior of vampire bats, the moving task of each node is generated.

Step 5: Calculate the COVR of WSNs and count the uncovered grids.

Step 6: All the nodes are traversed and their total virtual force is calculated. Taking sensor node S_i as an example, its total virtual force can be expressed as $F_S(i) = FA_S(i) + FB_S(i)$, where $FA_S(i)$ and $FB_S(i)$ are the virtual force of uncovered grids and distance virtual force, respectively. If the total virtual force of all the nodes is zero, proceed to *Step 8*, otherwise proceed to *Step 7*.

Step 7: Virtual movement of nodes under the action of total virtual force. If the total virtual force of node S_i is zero, then the position of the node is not updated, otherwise, it is updated according to (13).

$$\begin{cases} PS_X(i) = PS_X(i) + \frac{F_{SX}(i)}{F_S(i)} \times Step(t) \\ \quad \times \exp\left(-\frac{1}{F_S(i)}\right) \\ PS_Y(i) = PS_Y(i) + \frac{F_{SY}(i)}{F_S(i)} \times Step(t) \\ \quad \times \exp\left(-\frac{1}{F_S(i)}\right), \end{cases} \quad (13)$$

where $F_{SX}(i)$ and $F_{SY}(i)$ represent, respectively, the components of force $F_S(i)$ along the X and Y directions; and $Step(t)$ is the step length of a single iteration of the nodes, which is calculated as $Step(t) = MaxStep - \frac{t}{T_{max}} \times MaxStep$, where $MaxStep$ is the upper limit of the step length of a single iteration, t is the current virtual iteration round, and T_{max} is the upper limit of the virtual iteration rounds. With the increase in virtual iteration rounds, the coverage rate increases gradually. In order to avoid the oscillation of the COVR in the later virtual iteration rounds, the step length of a single iteration is decreased gradually with increasing virtual iteration rounds. If the virtual iteration round of a node exceeds the upper limit, *Step 8* is performed; Otherwise, return to *Step 6*.

Step 8: The control center determines the final positions of the nodes and broadcasts movement orders to the nodes for redeployment.

V. EXPERIMENTAL RESULTS

Considering that MATLAB, OPNET, etc., all can verify the performance of the algorithm, we pay more attention to the coverage effect and simplify the communication process in the research. Therefore, VB-IVFA is compared with COSH [17], VF-IALO [20] and HA [15] in terms of the coverage enhancement and moving distance optimization under the environment of Windows 10 and MATLAB 2016b. The parameters of the four algorithms are presented in Table II.

TABLE II
SIMULATION PARAMETERS

Category	Parameters	Value
General parameter	Monitoring area	1000m × 700m
	Sensing radius	N (35, 6)
	Number of nodes	219
	Discrete interval of grids	2m
COSH	Distance of single step movement	3m
	Number of iterations	2
	Sampling step	35m
VF-IALO	Number of iterations	50
	Population number	30
VB-IVFA	T_{max}	60
	MaxStep	0.5m/iter

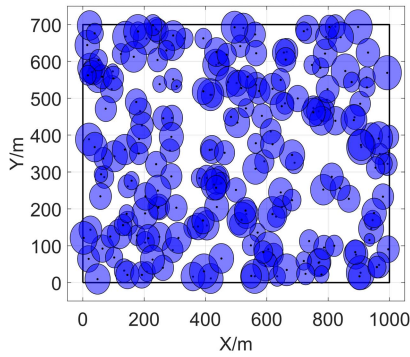


Fig. 10. Initial coverage effect.

A. Parameter Setting

As the key parameter of VB-IVFA, T_{max} and $MaxStep$ represent the upper limit of rounds of virtual iteration and the limit of the step length of a single iteration, which affects the final position of the nodes, thereby determining TMD and COVR of WSNs. In addition, $MaxStep$ and T_{max} affect the time-consuming of the algorithm, a small step length requires multiple iterations to find the optimal position of sensor nodes. If the step length is large, it is difficult to find the appropriate position to optimize TMD and COVR. Therefore, how to set the appropriate $MaxStep$ and T_{max} to realize the cost of redeployment and coverage effect optimization becomes the key problem. In this section, in the monitoring area of $1000m \times 700m$, different $MaxStep$ are set in the range of $10 \leq T_{max} \leq 100$ to count TMD and COVR, as shown in Table III. With the increase of T_{max} , the TMD under different $MaxStep$ is optimized and the optimization speed gradually slows down with the increase of T_{max} . With the increase of T_{max} , although TMD is excellent when $MaxStep = 2$, the COVR is limited. Considering the COVR, TMD, and time-consuming of the algorithm, the following simulation experiments will be carried out with $T_{max} = 60$ and $MaxStep = 0.5m/iter$.

B. Simulation Results and Analysis

A total of 219 nodes are deployed in the monitoring area of $1000m \times 700m$. Fig. 10 shows the initial coverage effect with COVR of 68.94%, and Fig. 11 shows the moving trajectory and final coverage effect of the considered four algorithms.

It is intuitive to see that VB-IVFA shows better performance in terms of COVR and TMD. Fig. 12 shows the plots of COVR of the four algorithms with the movement of nodes, where it is seen that for the initial COVR of 68.94%, the final COVR of COSH, VF-IALO, and HA are 92.75%, 94.47%, and 95.97%, respectively. The final COVR of VB-IVFA can reach up to 97.30%, which is 28.36% higher than the initial COVR, and 4.55%, 2.83% and 1.33% higher than those of the other three algorithms, respectively.

Based on the cellular grid division strategy, the uniformity in node distribution is guaranteed. Both HA and VBA enhance the final COVR by assigning 219 nodes to the 219 cellular grids on the basis of the cellular grid division strategy as presented in part III. For the coverage holes shown in Fig. 5, the virtual force of uncovered grids is proposed for further repairing of the coverage holes. The above considerations make VB-IVFA show a good coverage effect compared with HA. COSH takes TMD as the objective function to solve the position relationship between the sampling line and the virtual disk. However, the interval of the sampling lines is greatly affected by random deployment. It is difficult to find the optimal threshold in every experiment to increase the COVR. VF-IALO improves the COVR by combining VFA and ALO. However, as the number of nodes increases, it becomes difficult to allocate their weights for improving the COVR.

After the redeployment, the moving distance of each node of the four algorithms is shown in Fig. 13. The moving distance of the 219 nodes of VB-IVFA, HA, VF-IALO and COSH are shown from left to right. The MMD of COSH, VF-IALO, and HA are 285.97m, 132.37m, and 151.09m, respectively; while that of VB-IVFA is 111.54m, which is reduced by 60.99%, 15.74%, and 26.18%, respectively, compared with the former three. In addition, the UMD of VB-IVFA, COSH, VF-IALO, and HA are, respectively, 22.98m, 55.23m, 26.27m, and 30.27m, which manifest that VB-IVFA is 58.54%, 12.52%, and 24.08% lower than COSH, VF-IALO, and HA, respectively.

Fig. 14 shows the plots of COVR of the four algorithms with TMD. When the COVR of the four algorithms reaches 92.75%, the TMD of VB-IVFA becomes 7683.92m while COSH, VF-IALO and HA are 14098.82m, 12093.87m, and 8702.24m, respectively, which means that VB-IVFA needs a lesser moving cost under the premise of the same COVR. Similarly, when the nodes move the same distance, VB-IVFA can achieve a better COVR.

As a bipartite graph minimum matching algorithm, HA can obtain the minimum TMD once the cellular grid division strategy is determined, which is completely consistent with the goal of the egoistic behavior of VBA. However, the altruistic behavior of VBA balances the moving distance of nodes on the basis of minimizing the total moving distance by exchanging the moving task. Therefore, VBA has better performance in terms of MMD and UMD compared with HA. Additionally, the distance virtual force is proposed for further reduction of the TMD while optimizing the coverage effect. The contribution of the distance virtual force makes the TMD of VB-IVFA better than that of HA. Although COSH takes the moving distance as the objective function, it is difficult

TABLE III
THE INFLUENCE OF T_{max} AND $MaxStep$ ON THE TOTAL MOVING DISTANCE AND COVERAGE RATE

	$T_{max}=10$	$T_{max}=20$	$T_{max}=30$	$T_{max}=40$	$T_{max}=50$	$T_{max}=60$	$T_{max}=70$	$T_{max}=80$	$T_{max}=90$	$T_{max}=100$	
$MaxStep = 0.1m/iter$	COVR	96.21%	96.31%	96.40%	96.49%	96.57%	96.67%	96.73%	96.79%	96.84%	96.88%
	TMD/m	10730.46	10306.37	10275.71	10253.81	10229.72	10205.63	10179.15	10155.26	10131.17	10107.08
$MaxStep = 0.5m/iter$	COVR	96.53%	96.87%	97.05%	97.09%	97.12%	97.21%	97.15%	97.14%	97.07%	97.01%
	TMD/m	10238.48	10115.84	9997.58	9883.70	9774.21	9607.46	9574.91	9560.25	9512.76	9471.35
$MaxStep = 1m/iter$	COVR	96.85%	97.04%	97.12%	97.13%	97.01%	96.84%	96.71%	96.56%	96.44%	96.28%
	TMD/m	10128.98	9894.65	9684.41	9489.50	9312.11	9217.62	9153.08	9130.78	9086.85	9073.16
$MaxStep = 2m/iter$	COVR	97.12%	97.17%	96.87%	96.58%	96.30%	96.05%	95.87%	95.68%	95.55%	95.45%
	TMD/m	9916.55	9511.40	9171.95	8116.14	8893.82	8458.01	8289.38	8206.03	8176.15	8141.79

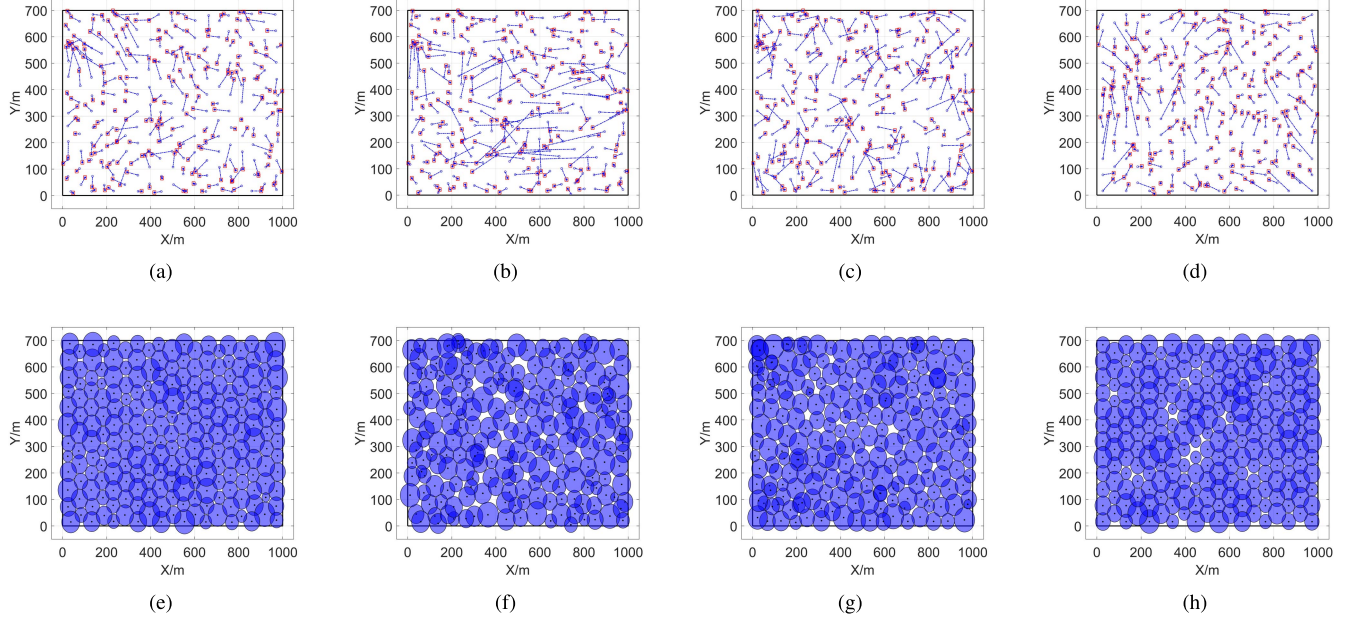


Fig. 11. Coverage of moving trajectory and final coverage effect of four algorithms. (a)–(d) and (e)–(h) are the moving trajectory and final coverage effect of VB-IVFA, COSH, VF-IALO and HA, respectively.

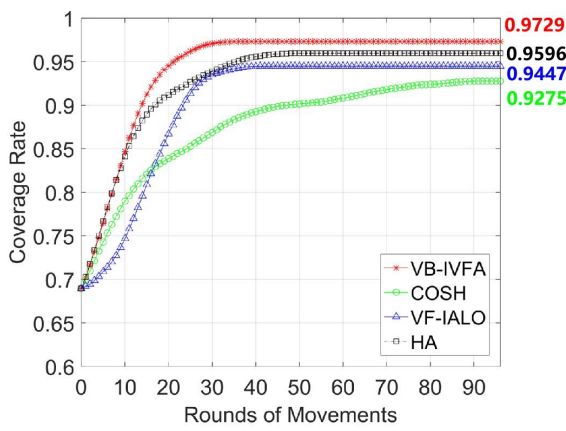


Fig. 12. The relationship between COVR and movement of nodes.

to avoid the local optimal solution when solving nonlinear optimization problems. In addition, COSH does not consider the UMD of WSNs. In order to control the moving distance, the position update of ants is restricted within an effective range from antlions. It solves the UMD partly, but cannot save the TMD for COVR.

TABLE IV
PERFORMANCE COMPARISON OF THE AVERAGE
RESULTS OF 200 EXPERIMENTS

PERFORMANCE	VB-IVFA	COSH	VF-IALO	HA
COVR	97.21%	91.78%	93.96%	95.58%
TMD/m	9607.46	14476.91	9972.45	9812.42
UMD/m	23.72	52.53	24.18	32.18
MMD/m	121.51	298.33	131.82	195.82

In order to verify the reliability of VB-IVFA, 200 experiments are performed independently with different initial positions, as shown in Table IV and Fig. 15. The average COVR of VB-IVFA, COSH, VF-IALO and HA are 97.21%, 91.78%, 93.96%, and 95.58%, respectively. The TMD of COSH, VF-IALO and HA are 14476.91m, 9972.45m, and 9812.42m respectively. The VB-IVFA proposed in this paper is only 9607.46m, which is 33.64%, 3.66%, and 2.01% lower than other algorithms. The UMD of VB-IVFA is reduced by 54.84%, 1.90%, and 26.29%, respectively. The MMD is reduced by 59.27%, 7.82%, and 37.95%, respectively. Multiple experiments can firmly verify the accuracy of a single experiment. We also make statistics on the time-consuming

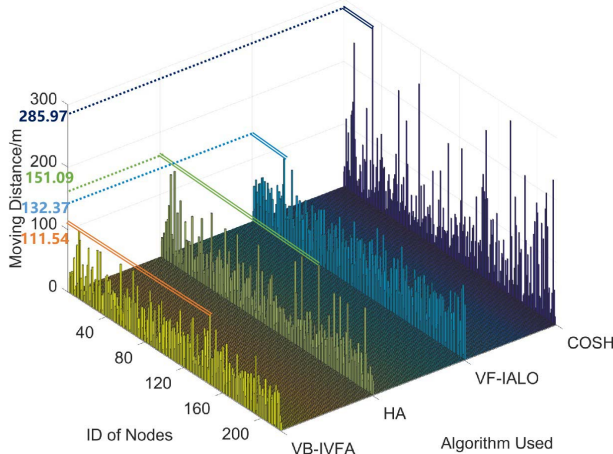


Fig. 13. Comparison of the moving distance of 219 nodes of four algorithms.

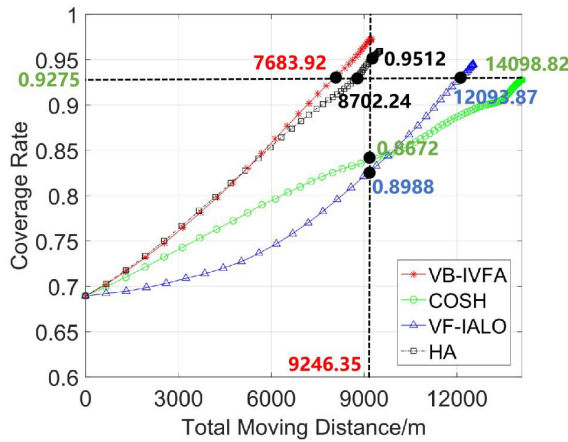


Fig. 14. Relationship between COVR and TMD.

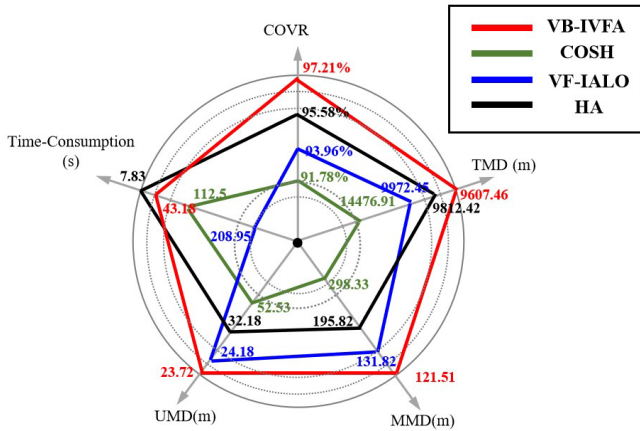


Fig. 15. Performance comparison of the average results of 200 experiments.

of the four algorithms. The average time consumption of VF-IALO, COSH and VB-IVFA are 208.95s, 112.5s, 43.18s. HA has the least time consuming, which is 7.83s. The main reason as follows, ALO is suitable for the optimization problem of high-dimensional functions, however, the time-consuming increases exponentially with the increasing

TABLE V
AVERAGE PERFORMANCE OF DIFFERENT δ UNDER 200 EXPERIMENTS

PERFORMANCE	$\delta = 3$	$\delta = 6$	$\delta = 9$
COVR	98.12%	97.21%	96.78%
TMD	9588.95	9607.46	10052.71
UMD	23.31	23.72	24.93
MMD	120.81	121.51	127.48

number of nodes, which causes the worst performance in time-consuming. COSH abstracts the coverage problem as a non-linear optimization problem, which inevitably affects the time-consuming. In the first stage, VB-IVFA abstracts the coverage problem into a bipartite graph matching problem, which not only improves the COVR, but also greatly improves the convergence speed of the algorithm. In the second stage, a reasonable *MaxStep* is set to control the time-consuming by analyzing the influence of virtual force on the COVR and TMD. However, VB-IVFA adds the second stage IVFA on the basis of task assignment to optimize the COVR and TMD, which is acceptable that HA shows good performance in time-consuming than VB-IVFA.

In order to evaluate the robustness of the VB-IVFA, for different δ , Table V shows the average value of performance in 200 experiments. According to the analysis of Table V, for different δ , the average COVR is above 96.50%. In terms of the TMD, the maximum range of difference between different δ is 463.73m. Considering the randomness of sensing radius is generated by the normal distribution, the nodes with larger sensing radius need to move further to repair the coverage hole once the coverage hole is caused by the nodes with small sensing radius. Therefore, on the basis of ensuring the COVR, the difference in the TMD is acceptable. In the same way, the UMD and MMD are less sensitive to the δ .

C. Computation Complexity Analysis

In this paper, we propose a coverage enhancement strategy of WSNs, which is composed of VBA and IVFA. For a WSNs with N nodes and M discrete grids, when the upper limit of rounds of virtual iteration is T_{max}^{VF} , the computation complexity of VBA and IVFA are $O(N^2)$ and $O(T_{max}^{VF} \times N \times M)$, respectively. Therefore the computation complexity of the proposed VB-IVFA is $O(T_{max}^{VF} \times N \times M)$ since the latter is obviously bigger than the former. Given the monitoring area and the sensing radius of nodes, the coordinate of the cellular grid can be obtained without iteration, and its complexity can be neglected. The computation complexity of VF-IALO and COSH are $O(T_{max}^{AL} \times N_{pop} \times N \times M)$ and $O(N_{samp} \times N^2 \times M)$, where T_{max}^{AL} , N_{pop} and N_{samp} are the number of iterations, the population size and the number of sampling steps, respectively. It is obvious to see that VB-IVFA is superior to VF-IALO in computation complexity. In addition, VB-IVFA is also better than COSH due to $N_{samp} \times N \gg T_{max}$ in the experiment. The computation complexity of HA is $O(N^3)$, which is better than VB-IVFA because N is much less than M . But it is affordable and worthwhile since VB-IVFA provides better performance in terms of coverage effect and moving distance.

VI. CONCLUSION

In this work, we have proposed VB-IVFA to solve the coverage enhancement problem of WSNs. In comparison to COSH, VF-IALO, and HA, it has superior performances in terms of coverage effect and energy consumption optimization during the deployment. We firmly believe that VB-IVFA is capable not only to achieve the coverage enhancement of WSNs, but also to solve the problem of minimizing the movement of target coverage and the problem of repairing the emergency coverage holes.

However, the research of this paper still has some limitations. As our future work, the difference in the sensing ability between nodes will be reflected based on the probabilistic sensing model, which is a more realistic extension of the Boolean sensing model. Additional, adjusting the grid size dynamically based on the position of obstacles will be another interesting future work.

REFERENCES

- [1] C. P. Chen *et al.*, “A hybrid memetic framework for coverage optimization in wireless sensor networks,” *IEEE Trans. Cybern.*, vol. 45, no. 10, pp. 2309–2322, Oct. 2015.
- [2] X. Liu, A. Liu, T. Qiu, B. Dai, T. Wang, and L. Yang, “Restoring connectivity of damaged sensor networks for long-term survival in hostile environments,” *IEEE Internet Things J.*, vol. 7, no. 2, pp. 1205–1215, Feb. 2020.
- [3] G. Han, X. Yang, L. Liu, W. Zhang, and M. Guizani, “A disaster management-oriented path planning for mobile anchor node-based localization in wireless sensor networks,” *IEEE Trans. Emerg. Topics Comput.*, vol. 8, no. 1, pp. 115–125, Jan. 2020.
- [4] M. Wang, L. Zhu, L. T. Yang, M. Lin, X. Deng, and L. Yi, “Offloading-assisted energy-balanced IoT edge node relocation for confident information coverage,” *IEEE Internet Things J.*, vol. 6, no. 3, pp. 4482–4490, Jun. 2019.
- [5] B. Khalifa, A. M. Khedr, and Z. A. Aghbari, “A coverage maintenance algorithm for mobile WSNs with adjustable sensing range,” *IEEE Sensors J.*, vol. 20, no. 3, pp. 1582–1591, Feb. 2020.
- [6] D. Izadi, J. Abawajy, and S. Ghanavati, “An alternative node deployment scheme for WSNs,” *IEEE Sensors J.*, vol. 15, no. 2, pp. 667–675, Feb. 2015.
- [7] N. Chauhan and S. Urooj, “Model of smart gas sensor with the application of neural network for the detection of gases in active environment,” in *Proc. Int. Conf. Comput., Power Commun. Technol. (GUCON)*, Sep. 2019, pp. 748–752.
- [8] Z. Ganev, “Investigating signal transmission between sensor nodes located in indoor environment,” in *Proc. Int. Conf. Automatics Informat. (ICA)*, Oct. 2020, pp. 1–6.
- [9] K. M. Awan, P. A. Shah, K. Iqbal, S. Gillani, W. Ahmad, and Y. Nam, “Underwater wireless sensor networks: A review of recent issues and challenges,” *Wireless Commun. Mobile Comput.*, vol. 2019, pp. 1–20, Jan. 2019.
- [10] S. J. Lee, Y. S. Moon, N. Y. Ko, H.-T. Choi, and J.-M. Lee, “A method for object detection using point cloud measurement in the sea environment,” in *Proc. IEEE Underwater Technol. (UT)*, Feb. 2017, pp. 1–4.
- [11] Q. Zhang, C.-Y. Chang, Z. Dong, and D. S. Roy, “TCSR: Target coverage mechanism for sensors with adjustable sensing range in WRSNs,” *IEEE Sensors J.*, vol. 22, no. 4, pp. 3756–3765, Feb. 2022.
- [12] Z. Zhou, C. Du, L. Shu, G. Hancke, J. Niu, and H. Ning, “An energy-balanced heuristic for mobile sink scheduling in hybrid WSNs,” *IEEE Trans. Ind. Informat.*, vol. 12, no. 1, pp. 28–40, Feb. 2016.
- [13] F. Zhou, J. Gao, X. Fan, and K. An, “Covering algorithm for different obstacles and moving obstacle in wireless sensor networks,” *IEEE Internet Things J.*, vol. 5, no. 5, pp. 3305–3315, Oct. 2018.
- [14] G. Sallam, U. Baroudi, and M. Al-Shaboti, “Multi-robot deployment using a virtual force approach: Challenges and guidelines,” *Electronics*, vol. 5, no. 3, pp. 34–49, 2016.
- [15] Z. Liao, J. Wang, S. Zhang, J. Cao, and G. Min, “Minimizing movement for target coverage and network connectivity in mobile sensor networks,” *IEEE Trans. Parallel Distrib. Syst.*, vol. 26, no. 7, pp. 1971–1983, Jul. 2015.
- [16] H. Mahboubi and A. G. Aghdam, “Distributed deployment algorithms for coverage improvement in a network of wireless mobile sensors: Relocation by virtual force,” *IEEE Trans. Control Netw. Syst.*, vol. 4, no. 4, pp. 736–748, Dec. 2017.
- [17] X. Y. Du, L. J. Sun, J. Guo, and S. Han, “Coverage optimization algorithm for heterogeneous WSNs,” *J. Electron. Inf. Technol.*, vol. 36, no. 3, pp. 696–702, 2014.
- [18] C. Zhang and L. Gong, “An improved force-based deployment algorithm for wireless sensor network,” in *Proc. IEEE 17th Int. Conf. Commun. Technol. (ICCT)*, Oct. 2017, pp. 946–950.
- [19] C. Luo, Y. Cao, G. Xin, B. Wang, E. Lu, and H. Wang, “Three-dimensional coverage optimization of underwater nodes under multi-constraints combined with water flow,” *IEEE Internet Things J.*, vol. 9, no. 3, pp. 2389–2375, Feb. 2022.
- [20] Y. Yao, Y. Li, D. Xie, S. Hu, C. Wang, and Y. Li, “Coverage enhancement strategy for WSNs based on virtual force-directed ant lion optimization algorithm,” *IEEE Sensors J.*, vol. 21, no. 17, pp. 19611–19622, Sep. 2021.
- [21] M. Song, L. Yang, W. Li, and T. A. Gulliver, “Improving wireless sensor network coverage using the VF-BBO algorithm,” in *Proc. IEEE Pacific Rim Conf. Commun., Comput. Signal Process. (PACRIM)*, Aug. 2013, pp. 318–321.
- [22] X. Zhao, Y. Cui, C. Gao, Z. Guo, and Q. Gao, “Energy-efficient coverage enhancement strategy for 3-D wireless sensor networks based on a vampire bat optimizer,” *IEEE Internet Things J.*, vol. 7, no. 1, pp. 325–338, Jan. 2020.
- [23] K. Saleem, A. Derhab, J. Al-Muhtadi, and M. A. Orgun, “Analyzing ant colony optimization based routing protocol against the hole problem for enhancing user’s connectivity experience,” *Comput. Hum. Behav.*, vol. 51, pp. 3540–3750, Oct. 2015.
- [24] K. Saleem, A. Derhab, M. A. Orgun, and J. Al-Muhtadi, “Analysis of the scalability and stability of an ACO based routing protocol for wireless sensor networks,” in *Proc. 12th Int. Conf. Inf. Technol.-New Generat.*, Apr. 2015, pp. 234–239.
- [25] J. Zhou, M. Xu, and Y. Lu, “Maximizing target coverage rate in wireless sensor networks based on clone adaptive glowworm swarm optimization,” in *Proc. IEEE Int. Conf. Intell. Appl. Syst. Eng. (ICIASE)*, Apr. 2019, pp. 12–15.
- [26] Y. Morsly, N. Aouf, M. S. Djouadi, and M. Richardson, “Particle swarm optimization inspired probability algorithm for optimal camera network placement,” *IEEE Sensors J.*, vol. 12, no. 5, pp. 1402–1412, May 2012.
- [27] Y. Yoon and Y.-H. Kim, “An efficient genetic algorithm for maximum coverage deployment in wireless sensor networks,” *IEEE Trans. Cybern.*, vol. 43, no. 5, pp. 1473–1483, Oct. 2013.
- [28] Z. Sun, G. Zhao, and X. Xing, “ENCP: A new energy-efficient non-linear coverage control protocol in mobile sensor networks,” *EURASIP J. Wireless Commun. Netw.*, vol. 2018, no. 1, p. 15, Dec. 2018.
- [29] Z. Sun, C. Li, X. Xing, H. Wang, B. Yan, and X. Li, “ k -degree coverage algorithm based on optimization nodes deployment in wireless sensor networks,” *Int. J. Distrib. Sensor Netw.*, vol. 13, no. 2, Feb. 2017, Art. no. 155014771769324.
- [30] X. Cai, P. Wang, L. Du, Z. Cui, W. Zhang, and J. Chen, “Multi-objective three-dimensional DV-Hop localization algorithm with NSGA-II,” *IEEE Sensors J.*, vol. 19, no. 21, pp. 10003–10015, Jul. 2019.
- [31] X. Zhao, H. Zhu, S. Aleksić, and Q. Gao, “Energy-efficient routing protocol for wireless sensor networks based on improved grey wolf optimizer,” *KSII Trans. Internet Inf. Syst.*, vol. 12, no. 6, pp. 2644–2657, Jun. 2018.
- [32] S. Zakariayi and S. Babaie, “DEHCIC: A distributed energy-aware hexagon based clustering algorithm to improve coverage in wireless sensor networks,” *Peer-Peer Netw. Appl.*, vol. 12, no. 4, pp. 689–704, Jul. 2019.
- [33] G. Carter and G. Wilkinson, “Food sharing in vampire bats: Reciprocal help predicts donations more than relatedness or harassment,” *Proc. Roy. Soc. B, Biol. Sci.*, vol. 280, p. 1753, Feb. 2013, Art. no. 20122573.



Qin Wen (Student Member, IEEE) was born in 1998. He is currently pursuing the master's degree with the Xi'an University of Posts and Telecommunications, Xi'an, China. His research interests includes the technology and application of the Internet of Things.



Xiao-Qiang Zhao was born in Xi'an, China, in January 1977. He received the Ph.D. degree from the Xi'an University of Technology. He is a Full Professor with the Xi'an University of Posts and Telecommunications, Xi'an. His current research interest includes the technology and application of the Internet of Things.



Hong Chang was born in 1981. She is a Lecturer with the Xi'an University of Posts and Telecommunications, Xi'an, China. Her research interests include information countermeasures, spectrum sensing, and communication signal processing.



Yan-Peng Cui (Student Member, IEEE) was born in 1994. He is currently pursuing the master's degree with the Xi'an University of Posts and Telecommunications, Xi'an, China. His research interests include the large-scale unmanned aerial self-organizing networks, radar communication integration, millimeter wave, and terahertz coordination.



Yao-Ping Zeng was born in 1975. He is an Associate Professor with the Xi'an University of Posts and Telecommunications, Xi'an, China. His research interests include wireless sensor optimization of network coverage and edge computing.



Yin-Juan Fu was born in 1977. She is a Lecturer with the Xi'an University of Posts and Telecommunications, Xi'an, China. Her research interests include radar frequency stealth technology and wireless sensor networks.